MRS Communications (2022) 12:917–923

https://doi.org/10.1557/s43579-022-00274-6

MRS Communications

Research Letter

On a novel approach to the thermogravimetric analysis of polymers: Polystyrene

Mircea Chipara, Department of Physics and Astronomy, College of Sciences, The University of Texas Rio Grande Valley, 1201 W. University Drive, Edinburg, TX 78539, USA
Karen Lozano, Department of Mechanical Engineering, College of Engineering and Computer Science, The University of Texas Rio Grande Valley, 1201 W. University Drive, Edinburg, TX 78539, USA
Dorina Chipara, Department of Physics and Astronomy, College of Sciences, The University of Texas Rio Grande Valley, 1201 W. University Drive, Edinburg, TX 78539, USA
Carlos Delgado, and Victoria Padilla, Department of Mechanical Engineering, College of Engineering and Computer Science, The University of Texas Rio Grande Valley, 1201 W. University Drive, Edinburg, TX 78539, USA

Address all correspondence to Mircea Chipara at **mircea.chipara@utrgv.edu**

(Received 7 January 2022; accepted 12 September 2022; published online: 23 September 2022)

Abstract

A novel equation that describes the temperature dependence of the residual mass fraction (as determined by thermogravimetric analysis) is derived, assuming that the dependence of the residual mass fraction on temperature has a sigmoidal shape. The equation allows the estimation of the sigmoidal activation energy solely from the experimental data at a single heating rate. The consistency with the isoconversional approach and the relationship between the Ozawa and sigmoidal activation energies are reported. The equation was successfully tested by the thermal degradation of atactic polystyrene at various heating rates. Both the thermograms and their derivatives are analyzed in detail.

Introduction

High-temperature exposure triggers degradation processes in polymers and polymer-based materials.[1,2] Thermogravimetric analysis (TGA) quantifies the evolution of the mass of materials as a function of temperature and time when subjected to various temperatures in different environments. The main ones are: (1) the inert environment (represented as the thermal degradation of materials in nitrogen, noble gases, or vacuum). In this environment, the polymer-based material does not interact (reacts chemically) with the environment at any temperature.[3–5] (2) The planetary(Earth) atmosphere (defined mainly as a combination of nitrogen and oxygen[6,7]). Interactions between the degrading polymer and the environment are possible, mainly at high temperatures. (3) The reactive environment (which implies chemical reactions or physical modifications due to the interactions between the components of the atmosphere and the materials under investigation). The standard example is thermal degradation in the oxygen atmosphere. Some authors include the Earth environment within the reactive environment. (4) The space environment(s) which may include radiation, and/or highly accelerated particles, and/or extreme temperatures.[8]

The isothermal TGA focuses on the evolution of the mass of the sample at constant temperature (usually above room temperature) as a function of time. The non-isothermal TGA emphasizes the evolution of the mass of the sample, as the temperature of the sample is raised in time (typically with a constant heating rate in time). While non-isothermal TGA reflects the dependence of the residual mass of the sample on both time and temperature, in most cases the as-recorded experimental dependencies (thermograms) are considered to represent the dependence of the residual mass on temperature. Within this manuscript, RMF will represent the residual mass fraction, assumed normalized to 100, and expressed as a percent. The manuscript focuses on the non-isothermal degradation of materials (polymers) in an inert (nitrogen) atmosphere. For such elementary degradation processes, there is a simple relationship between polymer conversion and RMF.

TGA is recognized as a standard experimental technique in the study of homopolymers,[9,10] polymer blends,[11] copolymers,[12] block copolymers,[13] polymer-based nanocomposites,[14] and metals with low melting temperature.[2,3] The simplest TGA thermogram (performed under an inert atmosphere) is recognized by its single sigmoidal shape representing the dependence of the RMF on temperature.[15–18] Mathematically, the associated sigmoid equation exhibits no extremum point, has a single inflection point, and is symmetrical (the inflection point is located at the inflection temperature, T_I, where it is expected that RMF is equal to 50%). For more complex materials, the sigmoidal shape may be distorted, and/or the thermal degradation may be represented by a convolution of several sigmoids.[19] High heating rates are stretching the thermograms, affecting their symmetry.[20] In TGA experiments performed under oxygen or reactive gases atmospheres, the temperature and time dependence of the mass is expected to be more complex.

The manuscript focuses on a semiempirical derivation of a novel equation that describes the evolution of the residual mass fraction versus temperature, in the degradation temperature

domain (i.e., in the vicinity of the inflection point) and demonstrates that the actual thermograms representing the temperature dependence of the RMF of a simple homopolymer—in this case, atactic polystyrene (PS)—at different heating rates is well fitted by the new proposed equation. The choice of PS is straightforward: Atactic polystyrene is a simple polymer, technically completely amorphous, with the glass transition temperature at or below 100°C[21] (decreasing as the average molecular weight is decreasing), which is well below the temperature at which the thermal degradation starts. The thermal degradation of polystyrene[22–24] and related (nano)composites[22,23] is well-documented. Thus, the phase transitions and modifications of PS are not located in the vicinity of the thermal degradation domain, resulting in very simple (clean) thermograms. Accordingly, it is easier to understand the limits and the advantages of the novel proposed equation by selecting such a simple and well-documented polymer.

The manuscript includes a detailed study of the parameters associated with the derivatives of the as-recorded thermograms (with respect to time or temperature). A particular emphasis is given on the importance of the inflection temperature T_I, the inflection RMF labeled as m_I (which is the residual mass fraction at the inflection point), the amplitude of the derivative of RMF versus temperature at the inflection temperature (which represents the highest RMF loss rate), and the width of the derivative of the RMF (with respect to the temperature) dependence on temperature (w_I). Many authors reported the temperature at which the RMF reached a certain value, frequently selected arbitrarily.[25,26] It is the authors' opinion that some of such (most frequently used) parameters have an empirical nature and consequently do not carry a physical significance. The physical meaning of the inflection temperature is that of the temperature at which the mass loss rate, v_I, is highest.[3] Hence, T_I and v_I are the coordinates of the inflection point. Usually, the inflection point is defined as a minimum, which can be converted into a maximum by multiplication with-1. Some authors prefer to use the empirically defined T_{50} or $T_{1/2,}$ which is the temperature at which the RMF is equal to 50% (half of the initial mass[26]). For a perfectly symmetrical degradation process with no residue $T_{50} = T_{1/2} = T_I$.

The onset temperature aims to eliminate from thermograms the first part, where contributions due to adsorbed gases or volatiles may be present.[26] The (extrapolated) onset temperature is defined by the intersection between the line representing the (constant) mass on the low-temperature side of the thermogram (extended to higher temperatures) and the tangent to the thermogram at the middle of the transition range (inflection temperature). The onset temperature is determined by the dependence of the RMF on the temperature, which does not generate a precise location of the inflection point. The offset temperature has an analogous definition and represents the crossing between the tangent to the thermograms at the middle of the transition range (i.e., the inflection point) and the constant (residual) RMF baseline on the high-temperature side of the thermograms. Within this manuscript, it is considered that the width of the derivative of the thermogram is also a well-defined quantity, more accurate that the onset and offset temperatures. Some authors defined the thermal degradation range as the part of the thermogram between the onset temperature and the offset temperature.

Mathematically correct and physically significant are also the inflection temperature and the extremum (maximum) RMF loss rate, which are the coordinates of the inflection point. This approach adds the width of the derivative of the thermogram as an additional parameter that may be accurately extracted and analyzed.[3] The inflection RMF may also be determined from the initial thermogram, either directly or after locating the inflection temperature from the graph representing the derivative of the thermogram (with respect to the temperature) versus the temperature.

Materials and methods

Atactic PS powder, with an average molecular weight $M_W = 650{,}000$ and $M_W/M_N = 1.06$ was purchased from Alfa Aesar and used as received. Thermogravimetric Analysis experiments were performed in a nitrogen atmosphere using a TG 209-Tarsus (Netzsch-Germany) instrument, in the range 50 to 1000°C. Different constant heating rates (1, 5, 10, 20, 30, and 40°C/min) were used to degrade the polymer thermally. The research reported here does not include Human or Animal subjects.

Results

Within the Supplementary Information section included with this manuscript, it was demonstrated that a simple single sigmoid equation is consistent with the most important models associated with the thermal degradation of materials. The proof presented within the Supplementary Information section is based on a novel semi-empirical approach to an equation capable of describing the thermograms, starting from an expression based on a "guessed" mathematical equation, known to have a sigmoidal shape. Specifically, it was assumed that both the temperature dependence of the RMF and the time dependence of the RMF are represented by single sigmoid-like dependencies.

The dependence of the residual mass fraction (expressed in %) on temperature (measured in °C), for the thermal degradation of polystyrene, at various heating rates ranging from 1 to 40°C/min is shown in the upper left panel of Fig. 1. This dependence is consistent with a single sigmoid-like shape, with negligible residues. The dependence of the RMF on the degradation time (measured in minutes), for the thermal degradation of polystyrene, at various heating rates ranging from 1 to 40°C/min are shown in the upper right panel of Fig. 1. This dependence is also consistent with a single sigmoid-like shape. In conclusion, the basic assumptions of the proposed model, that both the temperature and time dependencies of the RMF have a sigmoidal shape, are verified for the thermal degradation of PS.

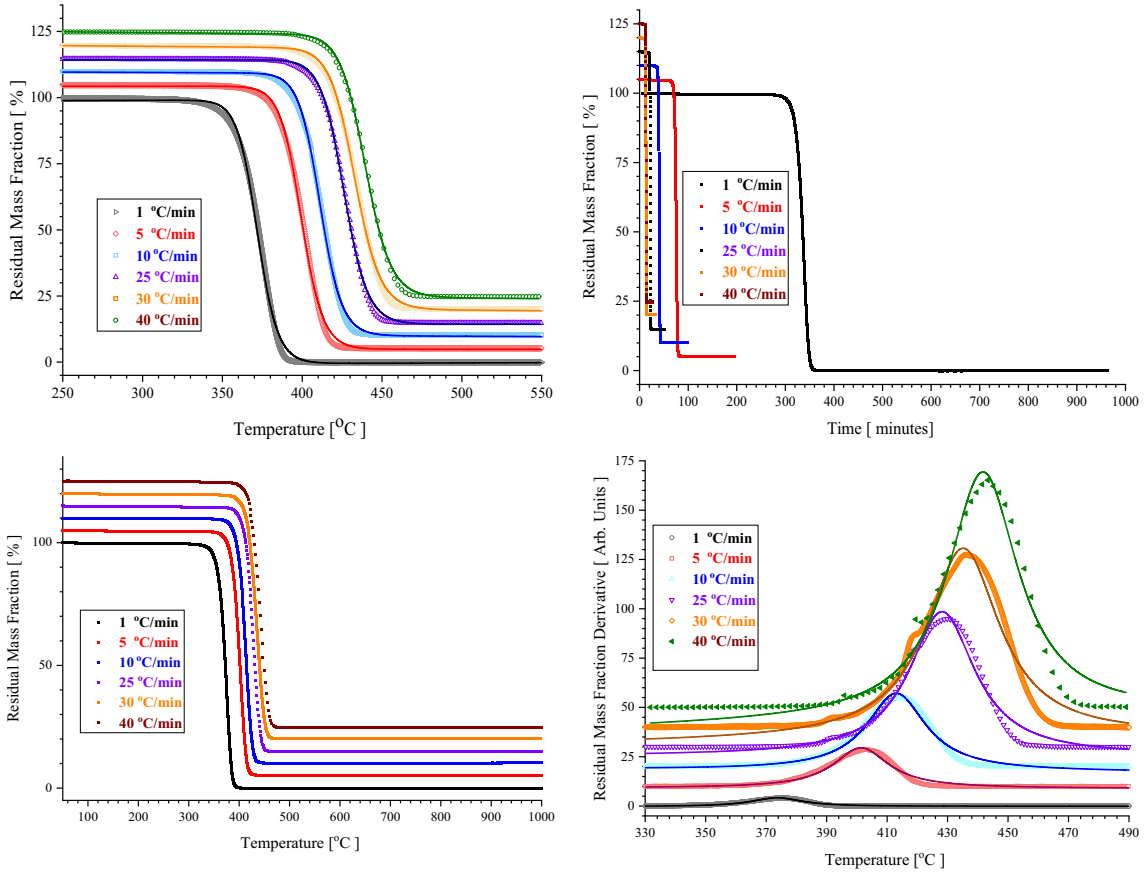

Figure 1. *TOP LEFT* The dependence of the RMF on temperature for PS degraded at various heating rates. *TOP RIGHT* The dependence of the RMF on the degradation time for PS degraded at various heating rates. *LOWER LEFT* The dependence of RMF on temperature, for different heating rates: Symbols are showing experimental data and the lines are the best fit obtained using Eq. (3). *LOWER RIGHT* The dependence of the temperature derivative of the RMF with respect to the temperature. Symbols show experimental data and lines represent the best fit obtained using the Eq. (4).

All thermograms shown in Fig. 1 have been shifted upwards by the same amount to allow for better viewing. The thermograms are shifted to higher temperatures as the heating rate is increased. It is observed that the number of data points per a given temperature range decreases as the heating rate increases. The inflection temperature shifts to higher values as the heating rate is increased, while the derivative of the thermogram narrows and its intensity is increased.

Some preliminary steps are required to continue further with the analysis of experimental data. As demonstrated in the Supplementary Information section, the thermograms are described by:

$$\Gamma^*(t,T) = \frac{A}{1 + B[\exp \alpha(t)]\left[\exp -\frac{|E_A|}{RT}\right]}, \qquad (1)$$

where $|E_A|$ was introduced to have the correct term (sign) for the Arrhenius component. Assuming that the temperature dependence of the RMF is stronger than the time dependence on the residual mass fraction, it is possible to neglect the time dependence (compared to the temperature one), within the degradation range.

This justifies the approximation $B\exp(\alpha t) \approx D$, where D is a constant. At this point is essential to notice that the complete separation of time and temperature is impossible. For this reason, it will be considered that this method provides the sigmoid activation energy, $E_A^{(S)}$, which may differ from the actual activation energy, E^A. Consequently, Eq. (1) becomes:

$$\Gamma^*(t,T) \approx \Gamma(T) = \frac{A}{1 + D\exp\left(-\frac{E_A^{(S)}}{RT}\right)}. \qquad (2)$$

The actual non-isothermal TGA data have been fitted using the expression within (Origin Pro):

$$C^*(\theta) = \frac{A_1}{1 + A_2\exp\left(-\frac{E_A^{(S)}}{8.3145(\theta+273.15)}\right)} + Z + S\theta, \qquad (3)$$

where $C^*(\theta)$ is the residual mass fraction at a given temperature θ, expressed in °C, $A_1 = A$, $A_2 = D$, Z is the baseline correction, S is the slope correction, and $E_A^{(S)}$ is the sigmoidal activation energy.

The lower left panel of Fig. 1 shows the dependence of the RMF on temperature for various heating rates. The symbols represent the experimental data and the lines the best theoretical predictions based on Eq. (3). It is concluded that the proposed model describes with good accuracy the experimental data.

The lower right panel of Fig. 1 represents the temperature dependence of the derivative of the residual mass fraction derivative (with respect to temperature). The symbols represent the experimental data and the lines the best fit obtained by fitting these dependencies using Eq. (4).

$$Y(\theta) = B + S \times x + (2 \times A/\pi) \times (W/(4 \times (\theta - G) \times (\theta - G) + W \times W)), \quad (4)$$

where Y is the intensity of the derivative of the thermogram at the temperature θ (where the temperature θ is in Celsius degree), B is the baseline correction, S is the slope correction, W is the width of the Lorentzian shape, A is the amplitude of the Lorentzian line, and G represents the temperature at which the maximum the derivative of the thermogram is reached.

For a symmetric sigmoid shape, it is expected for the residual mass fraction at the inflection point to be equal to 50%. The left panel of Fig. 2 represents the deviation from the symmetric sigmoid, defined as 50-m_I, where mI is the RMF at the inflection point. It is observed that this deviation is relatively low (about 5%). As expected the deviation increases as the heating rate is increased.

The proposed approach provides a path for the calculation of the so-called sigmoid activation energy, $E_A^{(S)}$ (see Eq. 3). Actually, within this model is possible to estimate the dependence of $E_A^{(S)}$ for each heating rate.

The dependence of the $E_A^{(S)}$ on the heating rate is shown in the right panel of Fig. 2. It is observed that the dependency of the sigmoidal activation energy on the heating rate is rather complex, exhibiting a maximum at a heating rate of about 10°C/min. The average sigmoidal activation energy is about 540,000 J/mole. The activation energy for the thermal degradation of polystyrene, calculated using the Coats-Redfern equation, was reported to be 263,000 J/mol.[21] The activation energy (for the thermal degradation of polystyrene) was found to range from 80,000 to 200,000 J/mol (increasing as the molecular mass is increased), with the highest molecular mass $M_n = 1.6 \times 10^6$.

This discrepancy was not unexpected and reveals why this activation energy was labeled as sigmoidal. The next step will tentatively focus on the estimation of the activation energy by standard methods for the PS degradation reported within the manuscript. Such an approach requires knowledge of the temperature derivative of the thermograms.

The temperature derivative of thermograms

In many cases, the as-recorded thermogram, i.e., the temperature dependence of the residual mass (fraction) is an envelope that engulfs several competing processes, even if the degradation process is represented by a single sigmoid.[21] Unexpectedly, some of these "hidden" thermal processes became visible if the derivative of the residual mass (fraction) versus temperature is represented as a function of temperature.[21] This explains why the derivative of the thermogram is considered in the analysis of TGA data.

In simple degradation processes, a single sigmoid-like thermogram is recorded. From the mathematical point of view, the thermograms have asymptotic behavior (are parallel to the horizontal axis) at the left and right extremities, have a single inflection point, and have no extreme value. The derivative of

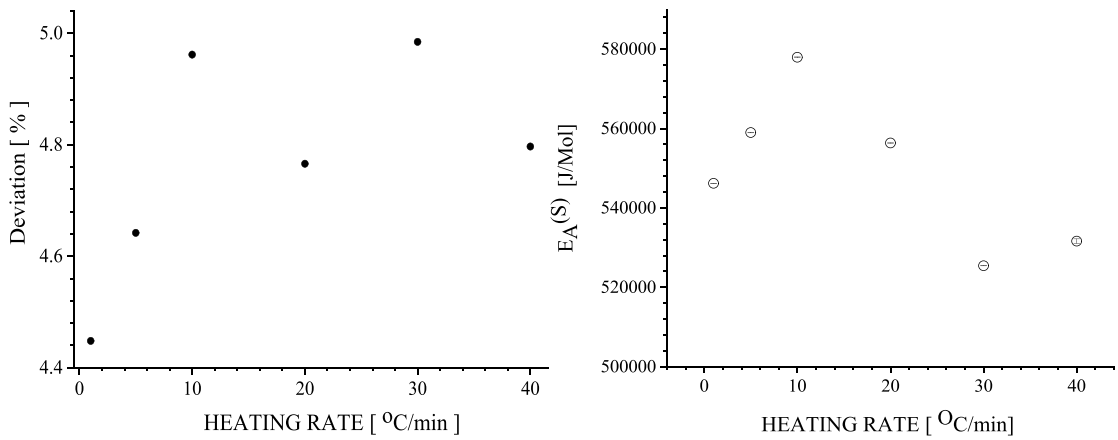

Figure 2. *LEFT* The deviation of the mass at the inflection temperature from the theoretical value for a symmetric thermogram. *RIGHT* Dependence of the sigmoidal activation energy on the heating rate for thermally degraded PS.

the thermogram with respect to the temperature should present a single maximum and two inflection points. These requirements define a broad class of functions, from which the Lorentzian will be considered for simplicity reasons.

As seen from the lower right panel of Fig. 1, the derivative of the thermogram versus temperature shows a very poorly resolved structure, suggesting that the degradation of PS is a more complex process. However, an acceptable agreement between the experimental data and the fit based on Eq. 4, was achieved.

From the left panel of Fig. 3 it is noticed that the inflection temperature, which is the temperature at which the RMF loss rate is maximum, increases linearly and monotonically as the heating rate is increased. The mass loss rate increases monotonically as the heating rate is increased, suggesting an asymptotic behavior at very large heating rates. The right panel of Fig. 3 depicts the dependence of the width of the thermogram's derivative on temperature. This width is increased as the heating rates increase from 1 to about 30°C/min, showing a maximum value at 30°C. The integral of the thermogram's derivative increases quasilinear as the heating rate is increased.

The left panel of Fig. 4 shows the dependence of the logarithm of the heating rate on the reciprocal temperature for various conversions. As expected, based on the theoretical approach discussed earlier, straight lines have been obtained. The correlation coefficient was about 0.98 for the 1% conversion and exceeded 0.99 for all (other) conversions, indicating an excellent agreement. The estimated activation energy depended on the conversion, increasing slowly as conversion increased towards 50% (see the right panel of Fig. 4). However, the estimated values of the activation energy were significantly lower than the values predicted using the sigmoidal approach.

There is a problem as the sigmoid activation energy differs significantly from what is reported. However, there are sufficient data to estimate the activation energy for our PS sample. Surprisingly, if it is assumed that $E_A = 0.456\ E_A^{(S)}$, a very good

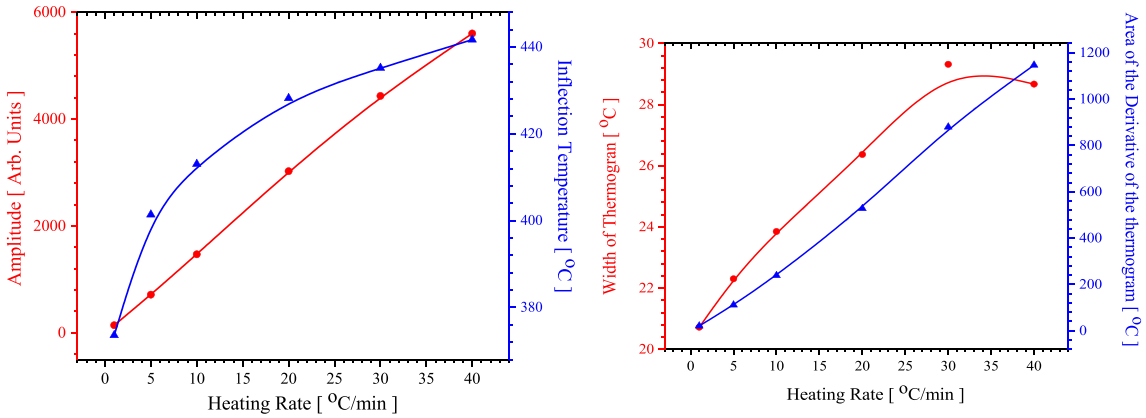

Figure 3. *LEFT PANEL* Dependence of the amplitude of the thermogram's derivative (highest RMF loss rate; left) and of the inflection temperature (right) on the heating rate. *RIGHT PANEL* Dependence of the width of the thermogram's derivative (left) and of the area of the thermogram's derivative on the heating rate (right).

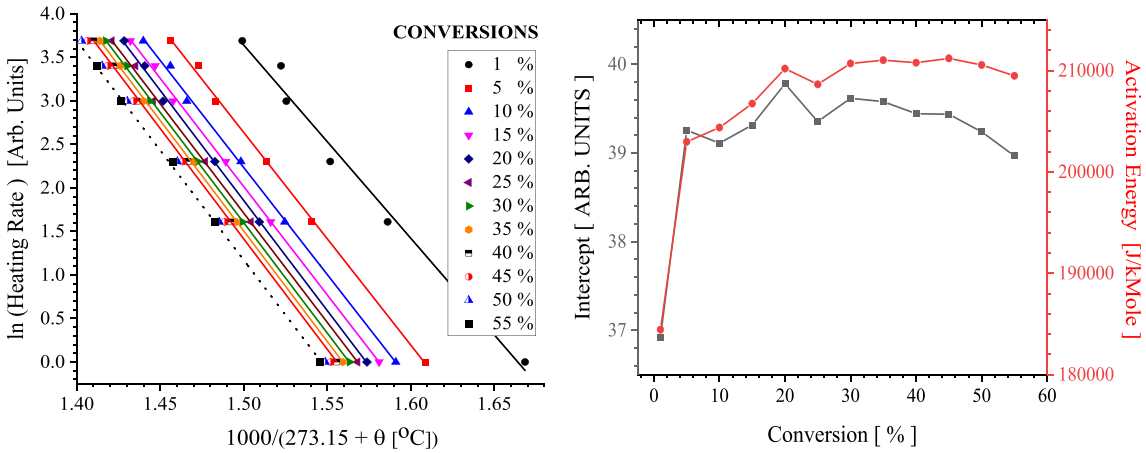

Figure 4. *LEFT PANEL* Dependence of the heating rate logarithm versus the reciprocal temperature, at various constant conversions. *RIGHT PANEL* Dependence of the activation energy on the conversion.

agreement between the sigmoidal and isoconversional activation energy. This is based on some isoconversion theories that estimate the slope of the dependence of the logarithm of the heating rates versus the reciprocal temperature to be 0.4567 E_A/R instead of E_A/R.[27]

Discussions

A novel theoretical equation for the temperature dependence of the residual mass is proposed. The original approach is based on sigmoid-like equations and starts from the assumption that in simple cases both the temperature dependence of the residual mass and the time dependence of the residual mass are expressed by sigmoid-like dependencies.

This assumption was successfully demonstrated in this manuscript. While the fact that the temperature dependence of the RMF was recognized earlier, this is for the first time when it is recognized that the time dependence of the residual mass fraction has also a sigmoidal shape. The approach allowed for the derivation of an original expression for thermograms, by exploiting the separation of variables method (with temperature and time as separable variables). The validity of this novel approach was demonstrated by the thermal degradation of polystyrene.

Subsequently, an equation for the temperature dependence of the residual mass is derived based on the sigmoid-like function. It is demonstrated that the new equation is capable of accurately describing the temperature dependence of the residual mass for PS degraded at various heating rates.

The activation energy (labeled as sigmoid activation energy) is derived from TGA data at each heating rate. It is observed that the sigmoidal activation energy depends on the heating rate.

The connection between the equation proposed, and the isoconversional theoretical approach to TGA is demonstrated.

The activation energy was estimated within the isoconversional theoretical approach. It was concluded that this activation energy depends on the conversion, showing a broad and flat maximum for a conversion of 50%.

It was noticed that the sigmoidal activation energy is larger than the isoconversional activation energy by a factor of about 2.0. This was explained in the Supplementary Inform by exploiting the Ozawa's interpretation[27] of the slope.

To conclude, the sigmoidal activation energy for atactic PS, calculated using Eq. (2), is consistent (within experimental errors) with the activation energy estimated using Ozawa's approach.[27] Additionally, it was shown that there is a very good relationship between the recorded experimental data and the predictions based on the proposed novel equation. These results support the novel semi-empirical equation, proposed to describe the temperature dependence of the RMF, derived within this manuscript. The manuscript also included a detailed analysis of the thermograms' derivatives. As expected, the agreement between the theoretical Lorentzian shape (for the dependence of the thermogram's derivative versus the temperature) and the experimental data are very good. This complementary analysis added the width of the thermogram's derivatives among the parameters that describe the thermal degradation process.

Future developments: The choice of PS allowed the study of a very simple thermal degradation process, in an inert atmosphere (nitrogen), accurately modeled by a single symmetric sigmoidal dependence. The novel proposed equation was successfully confirmed by this research. Future efforts will aim at a better understanding of the limits of this novel equation designed to describe the temperature dependence of RMF. The research will extend to include faster heating rates, which are frequently associated with asymmetric sigmoidal shapes (as thermograms are stretched due to the increase in the heating rates). Additionally, "multiple steps thermal degradation processes", which may be represented as a superposition of two or more sigmoids will be investigated in detail. A typical example of such multiple thermal degradation processes is represented by the thermal degradation (in a vacuum or inert atmosphere) of polyvinyl chloride.[28] Tentatively, future analysis will include also thermal degradation processes in air. Such data are of great importance for environmental applications.

Acknowledgments

This research was supported by the National Science Foundation, Division of Materials Research,-Partnership for Research and Education in Materials (PREM) Grant 2122178.

Data availability

All experimental data (graph and modeling/fitting) were processed using ORIGIN PRO including the C capabilities for data processing available within ORIGIN PRO. Experimental data as well as fitted data will be made available upon reasonable request.

Declarations

Conflict of interest

On behalf of all authors, the corresponding author states that there is no conflict of interest.

Supplementary Information

The online version contains supplementary material available at https://doi.org/10.1557/s43579-022-00274-6.

References

1. A.M. Shehap, Thermal and spectroscopic studies of polyvinyl alcohol/sodium carboxy methyl cellulose blends. Egypt. J. Solids **31**, 75–91 (2008). https://doi.org/10.21608/ejs.2008.148824
2. K. Chrissafis, K.M. Paraskevopoulos, S.Y. Stavrev, A. Docoslis, A. Vassiliou, D.N. Bikiaris, Characterization and thermal degradation mechanism of

isotactic polypropylene/carbon black nanocomposites. Thermochim. Acta **465**, 6–17 (2007). https://doi.org/10.1016/j.tca.2007.08.007
3. M. Chipara, K. Lozano, A. Hernandez, M. Chipara, TGA analysis of polypropylene-carbon nanofibers composites. Polym. Degrad. Stab. **93**, 871–876 (2008). https://doi.org/10.1016/j.polymdegradstab.2008.01.001
4. J. Qian, C. Fu, X. Wu, X. Ran, W. Nie, Promotion of poly(vinylidene fluoride) on thermal stability and rheological property of ethylene-tetrafluoroethylene copolymer. E-Polymers **18**, 541–549 (2018). https://doi.org/10.1515/epoly-2018-0057
5. V. Kuncser, D. Chipara, K.S. Martirosyan, G.A. Schinteie, E. Ibrahim, M. Chipara, Magnetic properties and thermal stability of polyvinylidene fluoride-Fe_2O_3 nanocomposites. J. Mater. Res. **35**, 132–140 (2020). https://doi.org/10.1557/jmr.2019.375
6. Y.T. Shieh, H.T. Chen, K.H. Liu, Y.K. Twu, Thermal degradation of MDI-based segmented polyurethanes. J. Polym. Sci. Part A Polym. Chem. **37**, 4126–4134 (1999). https://doi.org/10.1002/(SICI)1099-0518(19991115)37:22%3c4126::AID-POLA11%3e3.0.CO;2-A
7. A. Datta, R.I. Kelkar, P. Boroojerdian, S.K. Kulkarni, D. Monika, An FTIR and TGA study of the thermal oxidation of C60. Bull. Chem. Soc. Jpn. **67**, 1517–1521 (1994)
8. M. Chipara, D.L. Edwards, J. Zaleski, B. Hoang, B. Przewoski, S. Balascuta, Space environment effect on fluorinated polymers. Mater. Res. Soc. Symp. Proc. (2003). https://doi.org/10.1557/proc-792-r2.10
9. G.V. Theodosopoulos, C. Zisis, G. Charalambidis, V. Nikolaou, A.G. Coutsolelos, M. Pitsikalis, Synthesis, characterization and thermal properties of poly(ethylene oxide), PEO, polymacromonomers via anionic and ring opening metathesis polymerization. Polymers (Basel) (2017). https://doi.org/10.3390/polym9040145
10. D.K. Chattopadhyay, D.C. Webster, Progress in polymer science thermal stability and flame retardancy of polyurethanes. Prog. Polym. Sci. J. **34**, 1068–1133 (2009). https://doi.org/10.1016/j.progpolymsci.2009.06.002
11. Z. Ahmad, N.A. Al-Awadi, F. Al-Sagheer, Morphology, thermal stability and visco-elastic properties of polystyrene-poly(vinyl chloride) blends. Polym. Degrad. Stab. **92**, 1025–1033 (2007). https://doi.org/10.1016/j.polymdegradstab.2007.02.016
12. F. Bezgin, K. Demirelli, Synthesis, characterization and thermal degradation kinetics of photoresponsive graft copolymers. J. Thermoplast. Compos. Mater. **29**, 1135–1150 (2016). https://doi.org/10.1177/0892705714563114
13. A. Stanciu, V. Bulacovschi, V. Condratov, C. Fadei, A. Stoleriu, S. Balint, Thermal stability and the tensile properties of some segmented poly(ester-siloxane)urethanes. Polym. Degrad. Stab. **64**, 259–265 (1999). https://doi.org/10.1016/S0141-3910(98)00198-0
14. A.K. Nikolaidis, D.S. Achilias, Thermal degradation kinetics and viscoelastic behavior of poly(methyl methacrylate)/ organomodified montmorillonite nanocomposites prepared via in situ bulk radical polymerization. Polymers (Basel) (2018). https://doi.org/10.3390/polym10050491
15. F. Lin, C. Wu, D. Cui, Synthesis and characterization of crystalline styrene-b-(Ethylene-co-Butylene)-b-styrene triblock copolymers. J. Polym. Sci. Part A Polym. Chem. **55**, 1243–1249 (2017). https://doi.org/10.1002/pola.28489
16. A.R.R. Adhikari, K. Lozano, M. Chipara, J. Qualls, The effect of carbon nanofiber on the thermo-physical behavior of polyethylene oxide. J. Appl. Polym. Sci. **120**, 3574–3580 (2011). https://doi.org/10.1002/app.33542
17. C. Reverte, J.L. Dirion, M. Cabassud, Kinetic model identification and parameters estimation from TGA experiments. J. Anal. Appl. Pyrolysis **79**, 297–305 (2007). https://doi.org/10.1016/j.jaap.2006.12.021
18. J. Luo, M. Liu, J. Chen, J. Min, Q. Fu, J. Zhang, Effectively maintaining the disentangled state of isotactic polypropylene in the presence of graphene nanoplatelet. Polymer (Guildf) (2021). https://doi.org/10.1016/j.polymer.2021.123806
19. Z. Ahmad, N.A. Al-Awadi, F. Al-Sagheer, Thermal degradation studies in poly(vinyl chloride)/poly(methyl methacrylate) blends. Polym. Degrad. Stab. **93**, 456–465 (2008). https://doi.org/10.1016/j.polymdegradstab.2007.11.019
20. E. Apaydin-Varol, S. Polat, A.E. Putun, Pyrolysis kinetics and thermal decomposition behavior of polycarbonate—A TGA-FTIR study. Therm. Sci. **18**, 833–842 (2014). https://doi.org/10.2298/TSCI1403833A
21. T. Kurort, Y. Sekiguchi, T. Ogawa, T. Sawaguchi, T. Ikemusa, T. Honda, Thermal degradation of polystyrene. Nippon Kagaku Kaishi **1977**, 894–901 (1977). https://doi.org/10.1246/nikkashi.1977.894
22. S. Bourbigot, J.W. Gilman, C.A. Wilkie, Kinetic analysis of the thermal degradation of polystyrene-montmorillonite nanocomposite. Polym. Degrad. Stab. **84**, 483–492 (2004). https://doi.org/10.1016/j.polymdegradstab.2004.01.006
23. K. Chrissafis, D. Bikiaris, K. Chrissafis, D. Bikiaris, Can nanoparticles really enhance thermal stability of polymers? Part II: an overview on thermal decomposition of polycondensation polymers. Thermochim. Acta **523**, 25–45 (2011). https://doi.org/10.1016/j.tca.2011.06.012
24. J. Wu, T. Chen, X. Luo, D. Han, Z. Wang, J. Wu, TG/FTIR analysis on co-pyrolysis behavior of PE, PVC and PS. Waste Manag. **34**, 676–682 (2014). https://doi.org/10.1016/j.wasman.2013.12.005
25. D. Tabuani, W. Granelli, G. Camino, M. Claes, Polypropylene based carbon nanotubes composites: structure and properties. E-Polymers (2008). https://doi.org/10.1515/epoly.2008.8.1.1178
26. V. Stefov, M. Najdoski, G. Bogoeva-Gaceva, A. Buzarovska, Properties assessment of multiwalled carbon nanotubes: a comparative study. Synth. Met. **197**, 159–167 (2014). https://doi.org/10.1016/j.synthmet.2014.09.011
27. T. Ozawa, A new method of analyzing thermogravimetric data. Bull. Chem. Soc. Jpn. **38**, 1881–1886 (1965). https://doi.org/10.1246/bcsj.38.1881
28. M. Chipara, J. Cruz, E.R. Vega, J. Alarcon, T. Mion, D.M. Chipara, E. Ibrahim, S.C. Tidrow, D. Hui, Polyvinylchloride-single-walled carbon nanotube composites: thermal and spectroscopic properties. J. Nanomater. **2012**, 1–7 (2012). https://doi.org/10.1155/2012/435412